567

VOLUME 80 SEPARATE No. 567

PROCEEDINGS

AMERICAN SOCIETY
OF
CIVIL ENGINEERS

DECEMBER, 1954

FLOW EXPANSION AND PRESSURE RECOVERY IN FLUIDS

by Harold Tults

HYDRAULICS DIVISION

{Discussion open until April 1, 1955}

Headquarters of the Society
33 W. 39th St.
New York 18, N. Y.

PRICE $0.50 PER COPY

This paper was published at 1745 S. State Street, Ann Arbor, Mich., by the American Society of Civil Engineers. Editorial and General Offices are at 33 West Thirty-ninth Street, New York 18, N. Y.

FLOW EXPANSION AND PRESSURE RECOVERY IN FLUIDS

Harold Tults[1]

SYNOPSIS

Investigating the possibility of improving the pressure recovery in flow expansions, the writer observed visually the separation phenomena and measured the development of velocity profiles and pressure distribution in a gradual unilaterally expanding two-dimensional rectangular test canal with varied divergence from zero degrees to 20 degrees in range of Reynolds number 5×10^4 to 3×10^5.

Two characteristic phases of separation phenomena, "instant-stop" and "separation start", and their locations in expansion were measured and photographed by flashlights.

The analysis of the data for pressure variations in longitudinal and traverse direction gives considerable information on the mechanics of flow separation.

A simple analytical dependency is established between the angle of divergence and the rate of separation at which the maximum pressure recovery in each section occurs. This permits us to predict the optimum divergence for any required rate of gradual expansion.

Experiments on improvement of pressure recovery disclosed that the pressure efficiency may be improved considerably when the separation-endangered area is connected to a by-pass, which removes the retarded flow particles and carries those in the direction of the pressure drop into the approach canal.

Notation

The letter symbols used in this paper conform essentially to the American Standard Symbols for Hydraulics prepared by the Sectional Committee on Letter Symbols and Abbreviations for Science and Engineering and approved by the American Standards Association in January, 1942.

INTRODUCTION

One of the most difficult problems of hydraulic and aeronautic engineering is the expansion of flow with its increased losses and the tendency of the flowing medium to separate from the walls when the rate of divergence is too great.

The separation of flow occurs when:

1. The fluid due to its inertia cannot follow the abrupt boundary changes of the conduit.

---

1. Asst. Hydr. Engr., Pioneer Service & Eng. Co., Chicago, Ill.

2. The expanding flow is retarded by such locally acting counterforces as viscosity near the boundaries and gravity of the rising particles in the hydraulic jump.

If the retarding viscosity forces are not concentrated at boundaries but evenly distributed over the entire section, as in seepage flow through porous soils, the flow in expansion follows the potential pattern without separation.

3. Sometimes the separation may occur as a natural regulator of energy balance. In flume intakes of flow with too high content of kinetic energy, as observed in front of regulated weirs during floods, the separation constricts the actual flow passage and destroys the excessive kinetic energy to fit in with the conveyance capacity of the flume.

This paper is concerned with the separation phenomenon in gradual flow expansion in closed conduit.

The theoretical treatment of separation problems by G. Hamel[(1)][2], W. Tollmien[(2)], H. Blasius[(3)], and K. Pohlhausen[(4)] revealed that the ability of laminar flow to expand and perform energy conversion is very limited.

Engineering problems deal mostly with turbulent flows and even the possible laminar boundary layer turns to a turbulent one before the start of separation. The turbulent flow is able to undergo considerable expansion without visual evidence of separation. This characteristic of turbulent flow is attributed to the turbulent interchange of kinetic energy. Professor A. A. Kalinske[(5)] experimenting on energy loss in flow expansion found that the large-scale turbulence is more effective in energy interchange than the fine-grained one and that the amount of turbulent energy, which kind of energy itself cannot be recovered, is only a fraction of the total energy lost in the expansion.

Before the experiments by the writer and the results are discussed in detail, a brief review will be given of possibilities of improving pressure recovery in laboratory tests and in engineering application.

Improvement of Pressure Recovery

Among the methods employed to improve the pressure efficiency are: increase of turbulence, deflection of kinetic energy into the separation area and improved velocity distribution at entrance to expansion, which help to delay the occurrence of separation.

a) Increase of Flow Turbulence. The artificially generated turbulence is not self-sustaining, differing from natural so-called established turbulence constantly engendered by shear forces. Consequently, it is subject to early viscous attrition and, therefore, should be utilized immediately.

The experiments by K. Andres[(6)] revealed that a whirl disc, perforated by three circular openings, placed in front of a diffuser set the water into intensive large-scale whirling and improved the efficiency from 0.72 to 0.82. On the other hand, a screen, whose effective range because of small-scale turbulence is comparatively short, reduced the efficiency from 0.53 to 0.42.

The outflow from modern low-head hydraulic turbines, such as Kaplan turbines, has a very high kinetic energy content. Recovery of that energy would be much more imperfect if the large-scale turbulence generated by the vanes did not exist in the outflow. Due to this high-degree local turbulence a strong flow expansion and an efficient pressure recovery is feasible.

Another possibility to intensify the turbulent interchange of kinetic energy

2. Numerals in parentheses refer to corresponding items in Appendix.

is given by superimposition of a rotation upon the translation of flow, which obviously stimulates the turbulent activity near boundaries.

Mr. Andres and K. Peters[7] created rotation by vanes in an approach canal of diffusers and obtained an improvement of about 15- to 20-per cent.

The aforementioned experiments revealed that the rotation is very effective. However, for the production of rotation special guide vanes are necessary, which often are uneconomical to construct and are the cause of increased friction losses.

Existing rotation in turbine outflow may be most effective for pressure recovery in concentric-type draft tubes. In elbow-type draft tubes the direction of the rotation is partly opposite to the secondary motion in the form of a double spiral, inherent to the elbow flow, and some of the tangential energy will be destroyed. The flattening of the elbow section in a draft tube helps to suppress the inducement of secondary motion.

b) Deflection of Kinetic Energy. In hydraulic practice, deflectors are frequently applied which guide more kinetic energy to the endangered zones to help to avoid separation. A typical example is the splitter in the bend of the elbow-type draft tube.

An improvement, considering the flow separation in rotation-free expansion, may be obtained by secondary motion, which appears in its most intensive form in bends. The losses in the bends are attributed to local flow expansions at the concave wall near the entrance and at the convex wall near the outlet. The experiments by H. Nippert[8] on flow losses in bends reveal that the most efficient bends had the most intensively developed secondary motion.

c) Improved Velocity Distribution in Entrance Section. An effective means to improve the diffuser performance is to set a nozzle or contraction in front of expansion, or shorten the approach canal as much as possible. The high boundary velocity thus achieved or preserved helps to delay the occurrence of separation.

A. Riffart[9] improved the efficiency about 17 per cent by placing a nozzle in front of a diffuser.

J. M. Robertson and D. Ross[10] obtained an increase of efficiency of 5- to 7-per cent, reducing the length-diameter ratio of the preceding straight pipe to cone from 10 to 3.

Experimental Work by the Writer[3]

The most emphasis was laid on qualitative research to acquire the fundamental knowledge of internal mechanics of separation occurrence.

The experiments were carried out with the simplest instruments available in the war-destroyed laboratory at the Technical University of Karlsruhe in Germany during the years 1946-48.

Employment of unilaterally variable divergence for the flow expansion yielded the following advantages:

1. The flow, especially after the onset of separation, was more stabilized and it was possible to carry out more accurate measurements.
2. The measurements of static pressure could be accomplished conveniently at both walls, with pressure variation on the straight wall corresponding to pressure variation in the center-line of a symmetrical expansion.

3. Complete data submitted with a thesis to the Technical University of Karlsruhe in Germany in practical fulfillment of the requirements for the degree of Doctor of Engineering and filed for reference in the Library of said University.

3. It was possible to investigate the improvement of pressure recovery in analogous transitions as in the horizontal leg of the elbow-type draft tube.

Test Facility

The test canal, Figures 1 and 2, built into an hydraulic flume, consisted of a 29 foot long straight approach canal of 0.654 x 0.656 feet cross-section, of a two-dimensional expansible test canal 2.85 feet long and of an outlet 4.5 feet long. The outlet canal had a movable wall to a maximum width of 1.41 feet.

The bottom and the cover of the test canal were made of plate glass for visual observations. The angle of divergence could be enlarged from zero up to 20 degrees by turning one sidewall on pivots. The curve of transition had a radius of 15/16 inch.

The pressure variations along the walls were measured by 14 wall piezometers: I-IV in approach canal, 1-5 along the center-line of straight, and 1' - 5' along diverging wall and recorded in glass tubes on the tube bank by vernier-reading with an accuracy of 0.00033 ft. (0.1 mm). To reduce measurement errors in fluctuating flow areas, as many as ten readings were made and the results averaged.

For visual observations, tubes of 1/8-inch external diameter were inserted into the test canal through special guide tubes A, B, C, D and E, and red aniline-dye solution injected into the flowing water.

Velocity was measured near the end of expansion in the last piezometer section 5 by a differential vacuum Pitot tube mounted on a cross-sliding carriage, so that every filament of flow could be caught axially into the gauging tube.

The rate of flow was measured by means of a calibrated rectangular weir with semicircular crest.

The water for the experiments was supplied from a 1,400 cubic foot water tank with a constant surface level and recirculated by a pump of 2.8 cubic feet per second capacity.

Velocity Distribution

Employing the Pitot tube for velocity measurements would not give correct values in eddy-disturbed regions, but no other instruments were available at the time the tests were made.

There are two sources of inaccuracy: pulsations of flow and limited sensitivity of Pitot tube.

The varying instantaneous velocity "v" may be divided into components: temporal mean velocity $\overline{v}$ and local velocity fluctuations v'. $v = \overline{v} + v'$ (1)

The relative fluctuation $\frac{v'}{\overline{v}}$ varies from very small value in the entrance of expansion where turbulent uniform-flow pattern exists, to infinity at the separation point. It is clear that corrections of the Pitot tube indications are indispensable under such flow conditions. Unfortunately, such coefficients have not been established.

R. Kroner[11] compared the rates of flow measured by control weir and evaluated from contour plans of velocities measured by Pitot tube, and found the latter to be 5- to 10-per cent higher.

The sensitivity of the Pitot tube was limited by the least rate of vernier-reading of 0.00033 foot (0.1 mm), corresponding to a minimum measurable velocity of 0.14 foot per second.

As the gradient of mean velocity profile turns very gradually to zero in separation boundary, it was not possible accurately to establish the location of separation points employing the Pitot tube.

The pattern of variation of velocity profiles at divergence 0^o, 8^o, 12^o, 16^o, and 20^o in Figure 3 is typical for flow expansion at different flow rates. The standard profile of uniform turbulent flow grew more and more pointed with the increase of expansion. The reduction of velocity was strongest at the diverging wall, where the separation occurred.

The most important finding was that after the occurrence of separation, the width of forward flow remained almost constant. The additional increase of sections beyond the separation boundary just became filled by back flow.

Although the separation boundary remained unchanged, the disturbances as large-scale eddies intruded deeper into the forward flow, decelerating the adjacent flow filaments more and more. As the result from that and from added back flow rate, the maximum velocity and the velocity of flow in the opposite straight half of the conduit started to increase again.

The curvature of velocity profile on the diverging side of expansion turned convex exhibiting an inflexion point characteristic to the separation profile.

Pressure Variation

The measurements of static pressure along the walls were carried out for three different rates of flow: Q = 0.704, 1.407, and 2.110 cubic feet per second, corresponding to Reynolds numbers 1×10^5, 2×10^5, and 3×10^5, respectively.

The pressures were measured in reference to the piezometer II in approach canal 4.75 feet upstream from Section 1. The pressure recovery itself was computed in reference to the Section 1, reduced by the friction loss established for the uniform flow.

The pressure variations are plotted in dimensionless form in Figure 4:

$$\Delta\bar{p} = \frac{\Delta p}{V_1^2/2g} \qquad (2)$$

Δp = Pressure difference, measured from the start of the expansion.

V_1 = Mean velocity at entrance, ratio of discharge to area.

g = Gravitational acceleration.

The interpretation of the course of conjugated curve pairs in Figure 4, measured at straight and diverging wall, permitted the following conclusions to be drawn:

1. The pressure variations differ for each wall, especially at the entrance and outlet where the influence of the curvilinear transition flow predominates.

2. The cross-sectional pressure differences plotted in Figure 5 indicate that at divergence greater than about ten degrees, a positive pressure difference similar to the potential flow exists, as demonstrated by dotted curve obtained from flow net for 16 degree divergence. Thus, the pressure rise at separation wall blockades the supply of kinetic energy not only in longitudinal but even in traverse direction.

3. It is possible to recognize the advancement of back flow zone from these curve pairs. The reversed flow separates the forward flow from the wall, bending the flow filaments and creating additional centrifugal pressure. This is represented by the local curvature increase of pressure curve for diverging wall and by the increase of cross-sectional pressure difference which moves upstream with the advancing back flow.

4. The induced separation constricts the flow passage at the end of the canal. The flow filaments are straightened and thus the cross-sectional pressure difference reduced.

Further, the variation of medium pressures were derived graphically for Q = 0.704, 1.407, and 2.110 cubic feet per second for Sections 2, 3, 4 and 5 (perpendicular to the straight wall) and plotted against the angle of divergence, as shown in Figure 6. Each of the curves has an explicit vertex point which represents the highest possible pressure rise for the respective section. The interconnection lines of these vertex points are straight parallel lines.

In this assembly of curves there are also represented the pressure variations in piezometers: IV - 0.49 foot in front of the entrance, and in 1 and 1' of the entrance section.

The lines for maximum pressure rise at different Reynolds numbers along the expanding canal are plotted in Figure 12. These lines are very closely situated. The same Figure exhibits the separation boundary as a heavy dotted line obtained by visual observations (see next Section - Visual Study). Surpassing the optimum divergence, at which the maximum pressure rise occurs, the separation of flow from the wall is induced very soon as indicated by closeness of separation boundary.

The rectilinear and parallel course of lines for maximum pressure rise in Figure 6 evidently points to a simple law for calculation of optimum divergence:

$$\alpha_{opt} = \alpha_1 + \alpha_2 \Delta\bar{p} \tag{3}$$

which may be transformed using:

$$\Delta\bar{p} = \eta\Delta\bar{p}_i = \eta \frac{(V_1^2 - V^2)/2g}{V_1^2/2g} = \eta\left(1 - \frac{1}{e^2}\right) \tag{4}$$

$$\alpha_{opt} = \alpha_1 + \alpha_2 \eta\left(1 - \frac{1}{e^2}\right) \tag{5}$$

α_1, α_2 = Constant angles.

$\Delta\bar{p}$ = Dimensionless pressure difference.

$\Delta\bar{p}_i$ = Dimensionless ideal pressure difference measured from the start of the expansion.

η = Pressure efficiency.

V_1 = Mean velocity in entrance section.

V = Mean velocity in expanded section.

e = Area ratio of expanded section to entrance section.

The values of e and η for maximum pressure rise are computed and tabulated in Table 1.

As shown in Table 1, the efficiency for maximum pressure rise along the expanding canal for each R value is almost constant. The deviations are not systematic and therefore the use of average efficiency for each R (i.e. for each Q) is justified. Computing the angles α_1 and α_2 the equation for straight line of maximum pressure rise in $\Delta\bar{p}$- and α-coordinates is:

$$\alpha_{opt.} = \alpha_1 - 12.16^{o} \times \eta\left(1 - \frac{1}{e^2}\right) \tag{5a}$$

α_2 is constant, but α_1 differs slightly for each R value.

TABLE 1. Efficiency $\eta = \Delta\bar{p} \frac{e^2}{e^2-1}$ for Maximum Pressure Rise in Sections of Expanded Canal

Section	Distance x	Diverg. α_{opt}	Expanded Width b	Rate of Expansion $e = b/b_1$	Pressure Rise $\Delta\bar{p}$	Efficiency η	Efficiency $\eta_{aver.}$
			0.705 cfs.	$R = 1\times10^5$			
2	0.492	15.1	0.786	1.203	0.260	0.840	
3	0.984	13.6	0.892	1.364	0.393	0.844	0.843
4	1.476	12.6	0.984	1.505	0.469	0.840	
5	1.903	12.0	1.058	1.619	0.524	0.847	
			1.401 cfs.	$R = 2\times10^5$			
2	0.492	15.6	0.791	1.210	0.254	0.788	
3	0.984	14.2	0.899	1.376	0.381	0.802	0.785
4	1.476	13.2	0.998	1.528	0.450	0.732	
5	1.903	12.6	1.081	1.653	0.492	0.769	
			2.110 cfs.	$R = 3\times10^5$			
2	0.492	14.7	0.783	1.198	0.238	0.786	
3	0.984	13.3	0.886	1.356	0.355	0.778	0.778
4	1.476	12.4	0.978	1.497	0.432	0.780	
5	1.903	11.8	1.053	1.611	0.473	0.769	

For $R = 1 \times 10^5$ ($Q = 0.704$ cfs.) $\alpha_1 = 18.3^o$ and $\eta = 0.84$
For $R = 2 \times 10^5$ ($Q = 1.401$ cfs.) $\alpha_1 = 18.7^o$ and $\eta = 0.79$
For $R = 3 \times 10^5$ ($Q = 2.110$ cfs.) $\alpha_1 = 17.6^o$ and $\eta = 0.78$

The equation (5) makes it possible to compute the maximum divergence for required rate of expansion, exceeding of which would not yield any rise of pressure, but rather a drop caused by increasing eddy losses.

The physical meaning for α_1 is the divergence for the rate of expansion, e, equal to 1 (i.e. for entrance section), at which the maximum pressure line hits the entrance section. As visual observations indicated, the separation point jumped to the entrance actually at a divergence of about 18^o.

The other limit of divergence for e equal to infinity seems also to be a definite value determined by α_2 and η. Assuming that the efficiency of pressure recovery would not vary with the length of expansion, the maximum divergence for infinite expansion would be:

$\alpha_{opt} = 17.6^o - 12.16^o \times 0.78 = 8.1^o$ for $R = 1 \times 10^5$

$\alpha_{opt} = 18.7^o - 12.16^o \times 0.79 = 9.1^o$ for $R = 2 \times 10^5$

$\alpha_{opt} = 18.4 - 12.16 \times 0.84 = 8.0^o$ for $R = 3 \times 10^5$

Professor H. Rouse[12] states: "In fact, when the deceleration is very gradual (i.e. for boundary inclinations less than perhaps 4^o) the flow may be completely free from separation if the Reynolds number is sufficiently high (i.e. if the boundary layer is turbulent)."

Using the data in Table 1, the curves for maximum pressure rise are plotted with divergence and expansion rate as coordinates in Figure 7. Any expansion whose divergence angle and expansion rate are on the curve or in the area between curve and coordinates is separation-free.

Further, the writer used the results of pressure measurements for computation of efficiency of pressure recovery. In Figure 8 is presented the efficiency along the canal at $R = 3 \times 10^5$. The efficiency of pressure recovery is maximum at 8^o divergence and is essentially constant along the canal. It increases along the canal at smaller and decreases at greater divergence. The manner in which pressure efficiencies vary with the divergence angle is illustrated for three different Reynolds numbers in Figure 9. The maximum efficiency in a section occurs at somewhat smaller divergence than the absolutely highest pressure rise marked by double-circles.

The pressure efficiency, computed in this ordinary way, is smaller than the true energy efficiency, if the uneven velocity distribution is taken into account.

The true kinetic energy E_k in a flow section is:

$$E_k = \int^A \frac{\gamma \bar{v}^3}{2g} dA \qquad (6)$$

and the ratio C_e of the true kinetic energy to that based on the mean velocity is:

$$C_e = \frac{1}{A} \int^A \left(\frac{\bar{v}}{V}\right)^3 dA \qquad (7)$$

γ = Specific weight of fluid.
$\bar{v}$ = Temporal mean velocity at a point.
V = Mean velocity, ratio of discharge to area.
A = Area.

For turbulent flow in uniform conduit C_e is close to unit. But C_e exceeds the unit considerably in uneven velocity distribution as in expanding flow. The writer computed by graphical integration the C_e values from velocity contour plans at Q = 1.407 cubic feet per second, measured in cross-section 5, and obtained:

1. for uniform flow $C_e = 1.13$, and
2. for expanded flow with 12^o 30' divergence $C_e = 1.51$.

Computing with these ratios, the energy efficiency is 0.88, which is appreciably higher than pressure efficiency 0.79.

Actually some of this additional kinetic energy may be recovered as pressure in an outlet canal, where the uneven velocity profile may resume the normal pattern of uniform flow. G. N. Patterson[13] gives the required length of duct following a cone, where the pressure continues to rise, with two to six times the outlet diameter.

A practical application to recover such kinetic energy is employed in well-designed draft tubes by contraction of transition between vertical and horizontal legs. As measurements indicate, such contraction does not only improve the velocity distribution, but even yields a pressure rise instead of drop as normally expected.

Visual Study

The observation of movements of colored flow filaments has contributed much to the knowledge of the mechanics of separation. It gives immediate information about the motions in development of flow separation from wall. The characteristic phases of separation were fixed by flashlight photographs (Figures 10 and 11).

The development of flow to the separation and to the back flow was gradual and steady. The pulsations of colored thread of dye solution entering the flow from tubes may be designated as "flickers" (change of velocity) and "flutters" (change of direction). The frequency of flickers decreased with increasing expansion, but the amplitudes of movements turned higher and higher.

The first reliable marked phase of development of flow to separation was an instantaneous stoppage of flow filaments with instantaneous velocity $v = \overline{v} + v' = 0$. The interconnection line of all of these points along the expansion canal represents the so-called "instant-stop boundary." The measurement of distances of instant-stop boundaries from the wall at different divergences made it possible to represent the advance of disturbed region toward the forward flow.

As the visual study revealed, the location of the instant-stop boundary is not affected appreciably by the rate of flow at the same angle of divergence.

Figure 12 shows the locations of instant-stop boundaries at increasing divergence from 10^{o} to 20^{o}.

The instant stops beyond the boundary turned into instant back-strokes, whose duration and amplitude increased until a stage appeared, where the colored filaments pendulated up and down indicating the velocity $\overline{v} = 0$, and $v = \overline{v} + v' = v'$. This phase appoints the beginning of full separation and is designated as the "point of separation" on the wall and as "separation or back-flow boundary" between forward and back-flow. It is interesting that the development phases appear in the same succession along the wall as in the cross-section of sufficiently expanded flow canal.

The separation from the wall started at the downstream section E of expansion at about $\alpha = 12^{o}\ 30'$ and moved upstream with increasing angle of divergence. The local minor separation behind the sharp-curved entrance transition did not extend itself with the increase of divergence. The flow always recontacted the wall downstream at a distance of about 1 inch from the end of the transition curve until the advancing back flow joined it abruptly when the divergence exceeded 18^{o}.

No dependency of separation occurrence upon Reynolds number could be established by visual observations. The close invariability of the separation boundary, established by velocity measurements, was confirmed also by visual observations. The separation boundary is shown as a heavy dotted line in Figure 12. The curves for occurrence of maximum pressure rise and that for separation are about parallel in their middle course, as the maximum pressure rise takes place prior to the occurrence of separation. The ends of curves intersect in front of downstream transition. Obviously, the occurrence of separation near the outlet is influenced by induced centrifugal pressure in outlet transition, while the pressure continues to rise due to the conversion of uneven velocity profile to the normal one in the outlet canal.

The rate of expansion, e, in Figure 12, at which the separation occurs, is assumed to be a rational function of dimensionless distance, $\frac{x}{b_1}$, from entrance Section 1. The analytical equation for occurrence of separation in applied test canal is:

$$e_{sep} = 1 + 0.3001\left(\frac{x}{b_1}\right) + 0.0493\left(\frac{x}{b_1}\right)^2 - 0.0776\left(\frac{x}{b_1}\right)^3 + 0.0176\left(\frac{x}{b_1}\right)^4 \qquad (8)$$

$$\alpha_{crit} = \text{Arc Tan}\left\{0.3001 + 0.0493\left(\frac{x}{b_1}\right) - 0.0776\left(\frac{x}{b_1}\right)^2 + 0.0176\left(\frac{x}{b_1}\right)^3\right\} \qquad (9)$$

x = distance from expansion start.
b_1 = width of entrance section.

Further the writer observed the length and the duration of dye traces in the boundary layer after cutting off the inflow of dye solution. The dye traces on the bright surface of aluminum could be easily observed against the light. The adherent traces even floated laterally like flags in wind and started to decrease from upstream end down.

It was possible to record the length of dye traces up to 12 inches and duration up to 60 seconds at slow flow with $R = 5 \times 10^4$. The length and duration of dye traces was reduced by increasing velocity (i.e. R number), likewise by increasing divergence. No traces could be observed at the highest applied rate of flow Q = 2.11 cfs corresponding to $R = 3 \times 10^5$.

Secondary Motion

The presence of a secondary motion was recognized by paths of air bubbles below the plate glass cover and from flow-direction indicators fastened on the bottom of the test canal. Both indicated that the flow direction near the cover and bottom had a greater angle to the straight wall than the angle of divergence.

In contour plans of velocity the secondary motion caused inward pockets near the separation wall and outward pockets at the opposite wall. The course of contour line for velocity equal to zero displayed distinctly the accumulation of retarded flow particles in the center of the divergence wall.

Improvement of Pressure Recovery

The pressure measurements displayed a rash increase of losses after the occurrence of separation. Any reduction of the highly strained discontinuity zone between forward and back flow would be very effectual means for the improvement of pressure conversion.

For that purpose three rows of openings (see Figure 13) were drilled into the diverging wall between piezometers 2' and 3'. Connecting these openings in the separation-endangered area with the approach canal by means of a by-pass conduit, a flow in the direction of pressure drop was induced. This self-acting back-flow drew off the retarded flow particles from the separation area and carried them into the approach canal.

At first, the entry into the approach canal was arranged on the shortest route in front of piezometer 1'. The result was adverse, because the entering fluid particles slowed down the boundary velocity and induced an early separation occurrence at about 3^o smaller divergence.

Connecting the by-pass to the other side of the entrance section in front of piezometer 1, a marked improvement of pressure conversion was obtained. Figures 14, 15 and 16 demonstrate the efficiency of the by-pass manipulation. The curves are plotted from expansions with open and closed by-pass to obtain the comparative data of improvements due to the by-pass action. Figure 14 shows the displacements of velocity distribution at divergence 14, 16 and 18 degrees. Some of the kinetic energy in the boundary layer was consumed by acceleration of entering back-flow particles. As the result of reduction of velocity at straight wall, the flow was deflected toward the separation area.

In Figures 15 and 16 the pressure recovery and efficiency are plotted, respectively. The pressure recovery due to the acceleration losses was reduced in the first part of expansion in front of draw-off openings. But the redistribution of kinetic energy downstream of draw-off not only effected a compensation of initial loss, but even increased the pressure recovery considerably. The

applied setup gave the best effect at 16^{o} divergence, increasing the pressure recovery about 16 per cent and efficiency from 0.55 to 0.66. The rate of draw-off was estimated by timing the passage of colored water through the by-pass and was found to be only 0.5 per cent of the total rate of flow.

CONCLUSIONS

The unilateral expansion created stabilized conditions for visual observations and measurements of the separation phenomena. The analysis of the test data allowed the following conclusions to be drawn:

1. The process of separation development is gradual and steady. The flow fluctuations at the diverging wall increase in amplitude, but decrease in frequency.
2. It is possible to determine by visual observations two characteristic phases of separation: (a) the "instant-stop boundary" with momentary velocity equal or greater than zero; and (b) the "separation or backflow boundary" with mean velocity equal to zero.
3. The same succession of phases of separation as along the wall exists also in sections across the flow.
4. The separation boundary did not vary with angle and with Reynolds number in the applied range. That itself is the principal condition for independency of Reynolds number. Yet the more accurate measurements of pressure variation in Figure 6 displayed only a partial conformity for $R = 2 \times 10^5$ and 3×10^5. Obviously, the pattern of boundary layers at lowest R number was still laminar, as observations of dye traces on the wall hinted.
5. The occurrence of separation in any section is preceded very closely by the occurrence of maximum pressure rise. For prediction of maximum pressure rise a simple quadratic relation (Eq. 5) is established between the optimum divergence and the rate of expansion required.
6. The energy recovery is considerably higher than the pressure recovery. The difference is presumably highest at the fully developed separation profile before the start of back flow. Some of this excessive kinetic energy may be recovered as pressure in an expedient outlet canal.
7. The minor separation, located behind the abrupt boundary change of entrance, could be avoided by flattening the transition curve. Any disturbance in that crucial section of entrance may decrease the boundary velocity and increase the expansion loss.
8. The pocket-like shape of velocity contour lines near the separation wall revealed that the induced secondary motion is pushing the slackened flow particles toward the center of the wall and is able to delay the separation, at least in the corners of the conduit.
9. Connecting the separation-endangered area with a by-pass conduit to the approach canal, it is possible to postpone the occurrence of separation and improve the pressure efficiency.

ACKNOWLEDGMENTS

The writer is indebted to Professor Paul Boss, Director of the Theodor Rehbock's River Laboratory of the Technical University of Karlsruhe for advice and assistance, and to the Educational Fund of Estonians in Refuge for the financial contribution that enabled the construction of the test canal.

REFERENCES

1. Spiralförmige Bewegungen Zäher Flüssigkeiten, by G. Hamel, Jahresbericht der Deutschen Mathematiker Vereinigung, Band 25, 1916.
2. Grenzschichttheorie, by W. Tollmien, Handbuch der Experimentalphysik, Band IV, 1. Teil.
3. Die laminare Strömung in erweiterten Kanälen, by H. Blasius, Zeitschrift für angewandte Mathematik und Physik, Band 58, 1910.
4. Zur näherungsweisen Integration der Differentialgleichungen der laminarer Reibungsschicht, by K. Pohlhausen, ibid., Band 1, 1921.
5. Conversion of Kinetic to Potential Energy in Flow Expansions, by A. A. Kalinske, Transactions, ASCE, Vol. III, 1946, pp. 355-390.
6. Versuche über die Umsetzung von Wassergeschwindigkeit in Druck, by K. Andres, Forschungsarbeiten des Vereins Deutscher Ingenieure, Heft 76, 1909.
7. Conversion of Energy in Cross-sectional Divergences under Different Conditions of Inflow, by H. Peters, Ingenieur-Archiv, Vol. II, 1931 (translated in Technical Memorandum No. 1137, National Advisory Committee for Aeronautics, 1934).
8. Über den Strömungsverlust in gekrümmten Kanälen, by H. Nippert, Forschungsarbeiten des Vereins Deutscher Ingenieure, Heft 320, 1929.
9. Versuche mit Verdichtungsdüsen, by A. Riffart, ibid., Heft 257, 1922.
10. Effect of Entrance Conditions on Diffuser Flow, by J. M. Robertson, and Donald Ross, Proceedings, ASCE, Separate No. 141, July, 1952.
11. Versuche über Strömungen in stark erweiterten Kanälen, by R. Kröner, Forschungsarbeiten des Vereins Deutscher Ingenieure, Heft 222, 1920.
12. Engineering Hydraulics, by Hunter Rouse, John Wiley & Sons Inc., New York, 1951, p. 118.
13. Modern Diffuser Design, by G. N. Patternson, Aircraft Engineering, 1938, p. 267.

Fig. 1. Test Canal and Measurement Instruments.

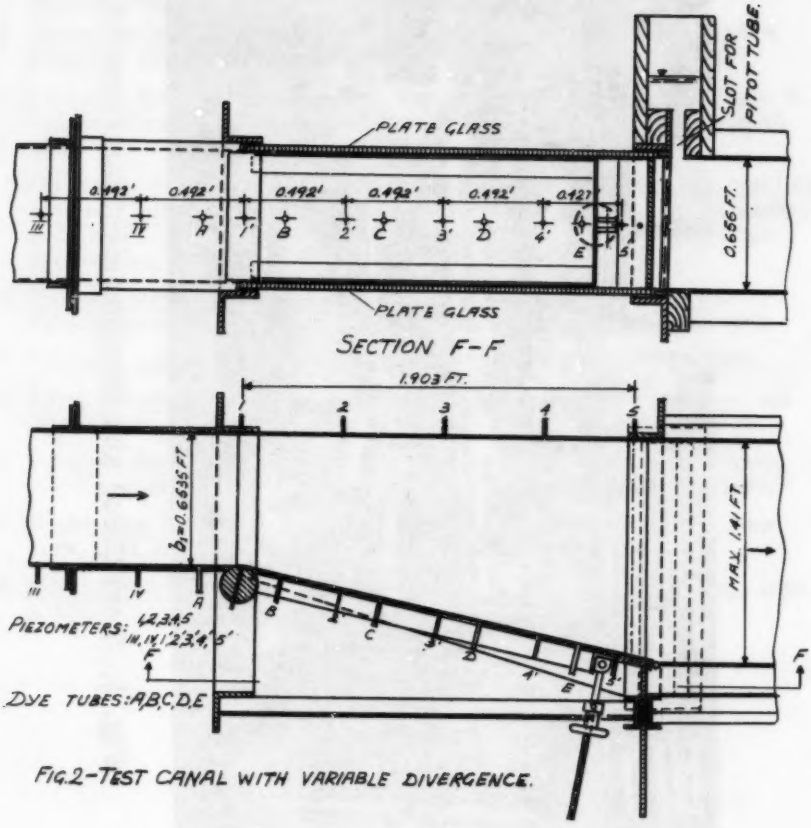

FIG.2-TEST CANAL WITH VARIABLE DIVERGENCE.

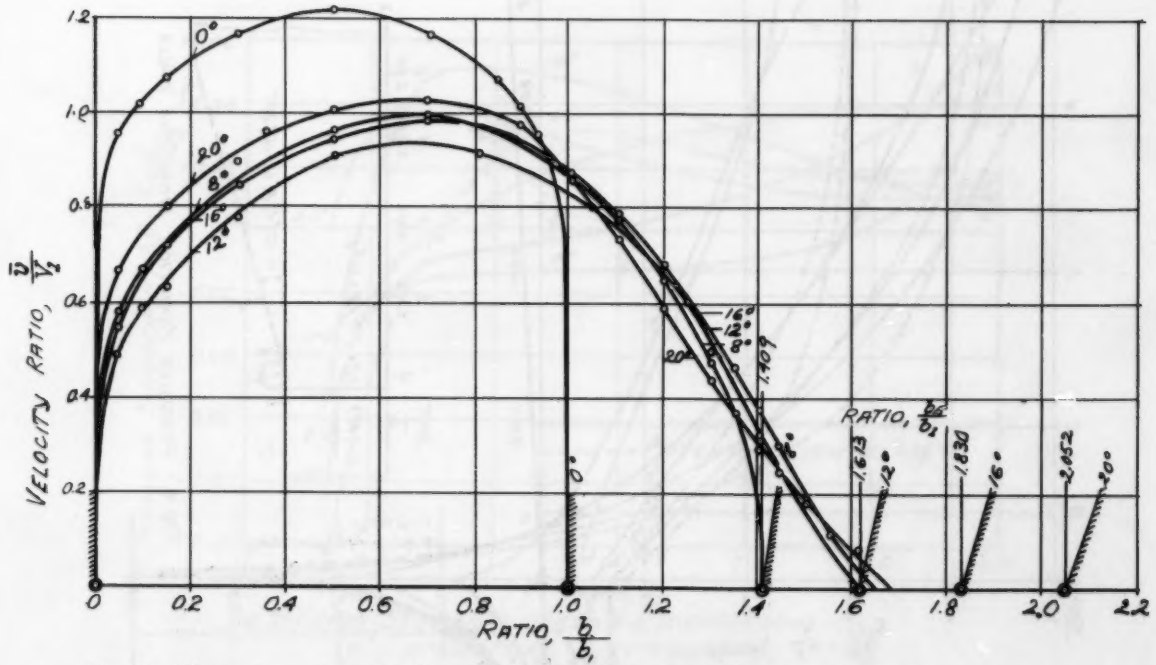

FIG. 3- VELOCITY PROFILES AT DIVERGENCE 0°, 8°, 12°, 16°, AND 20°

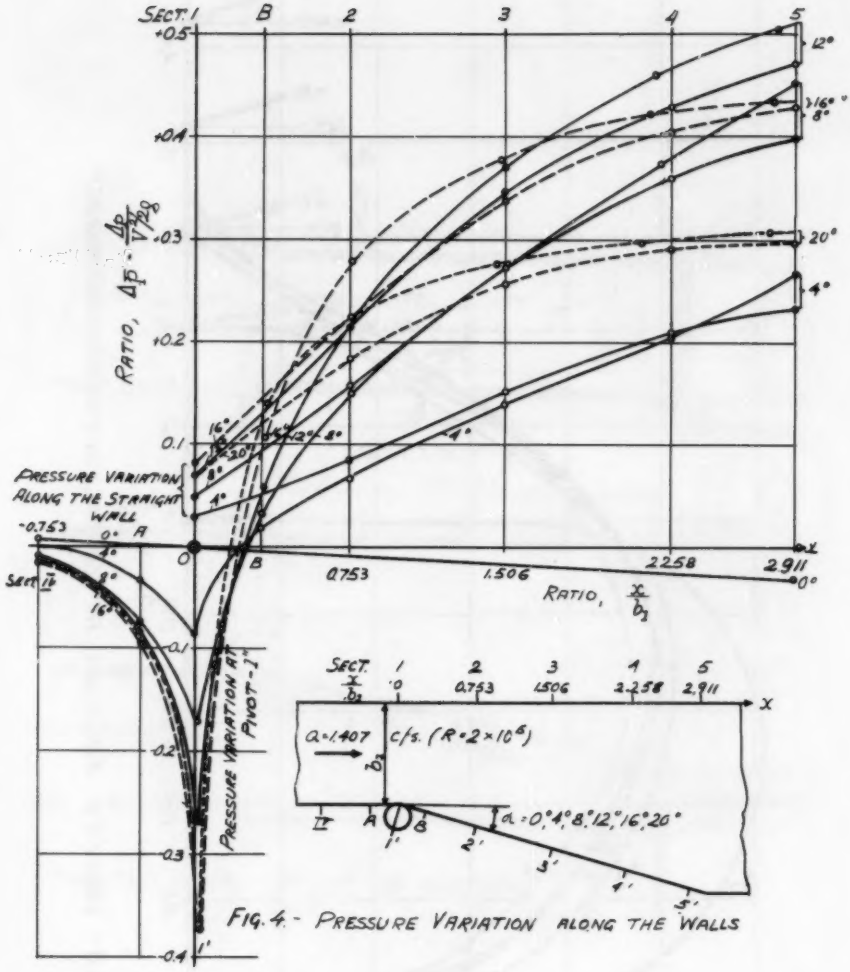

FIG. 4 - PRESSURE VARIATION ALONG THE WALLS

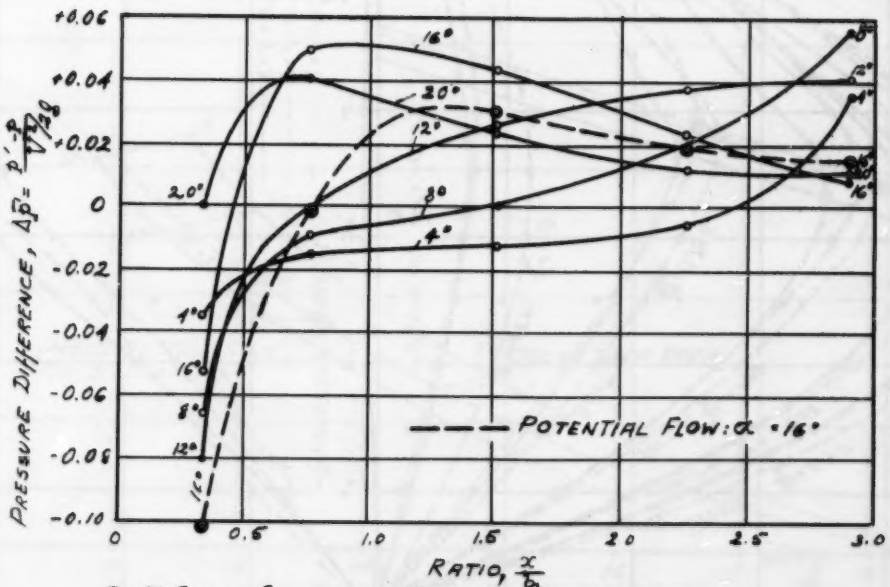

FIG. 5:-CROSS-SECTIONAL PRESSURE DIFFERENCES.
p'- pressure at diverging Wall
p- " " straight "

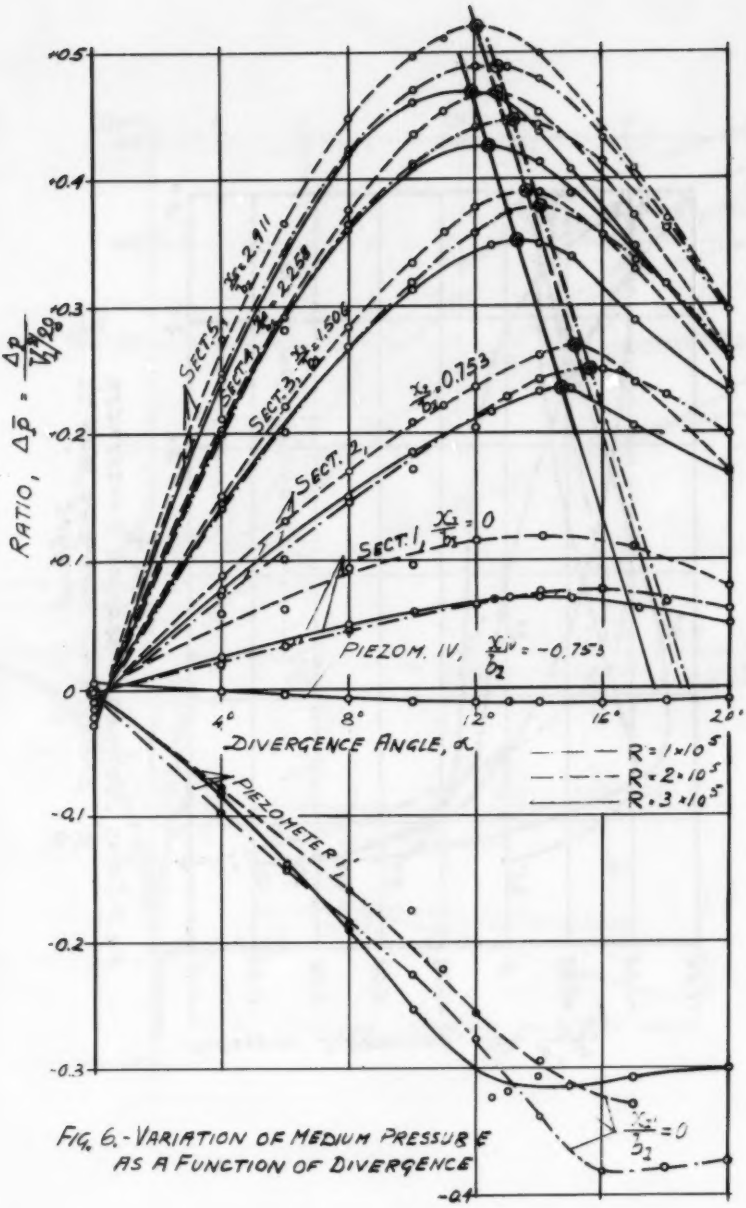

FIG. 6. - VARIATION OF MEDIUM PRESSURE AS A FUNCTION OF DIVERGENCE

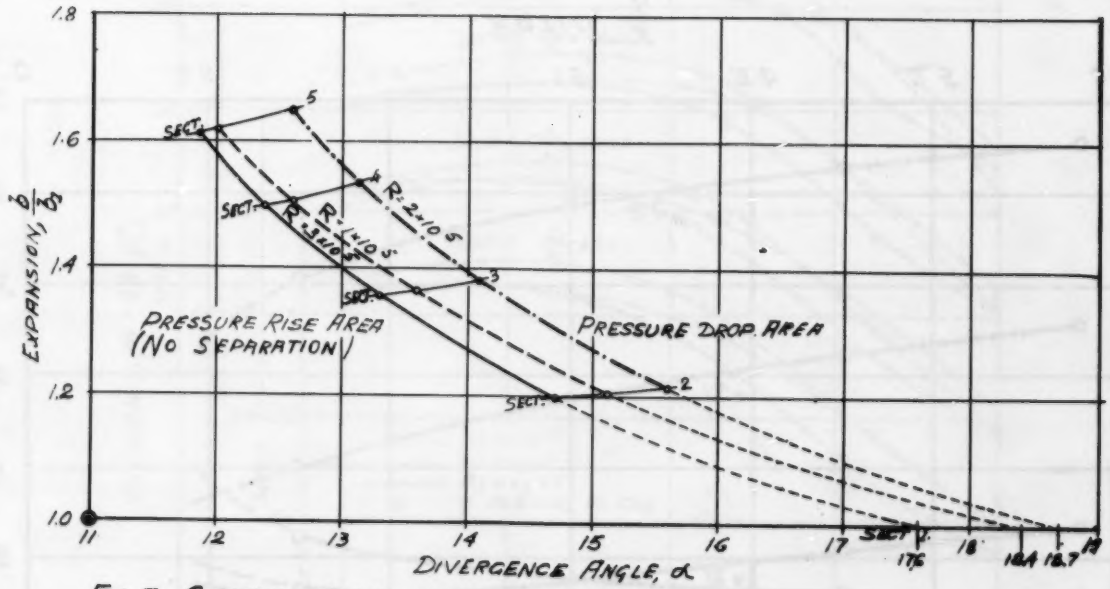

FIG. 7. - CURVES OF MAXIMUM PRESSURE RISE.

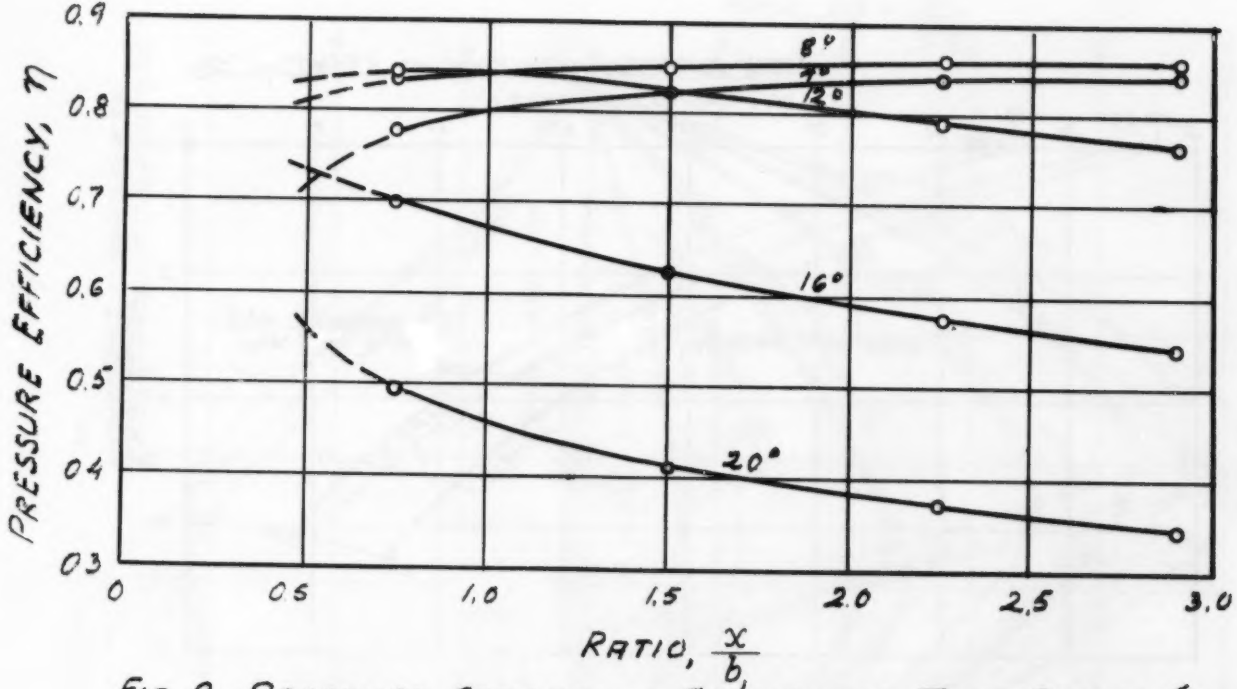

FIG 8.-PRESSURE EFFICIENCY ALONG THE TEST CANAL ($R = 3 \times 10^5$)

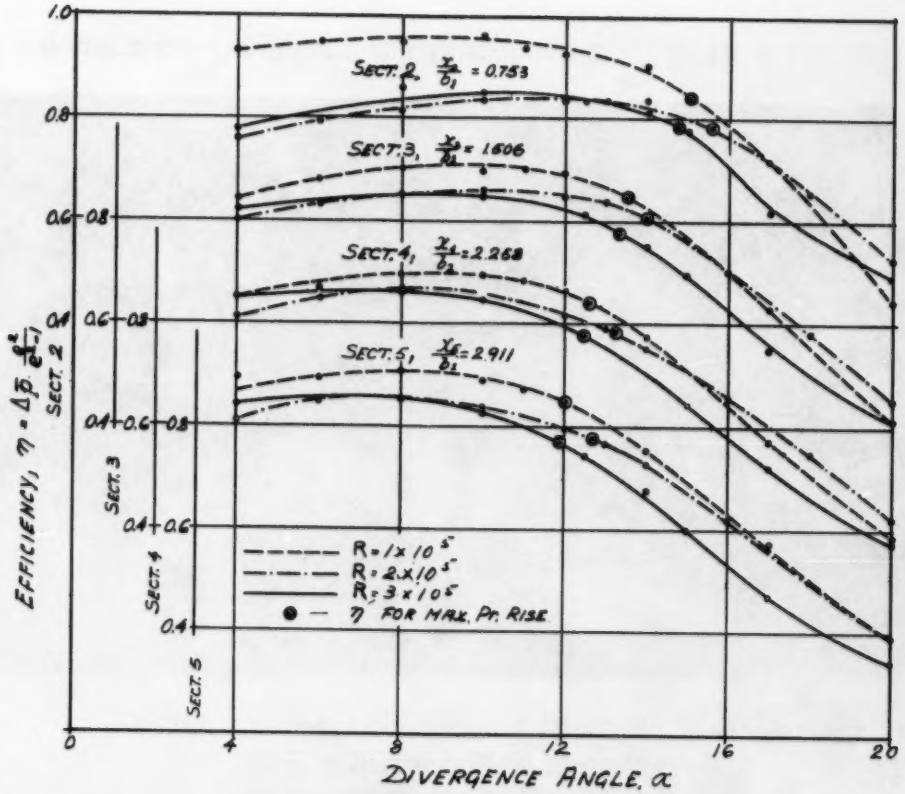

FIG. 9.- PRESSURE EFFICIENCY AS A FUNCTION OF DIVERGENCE

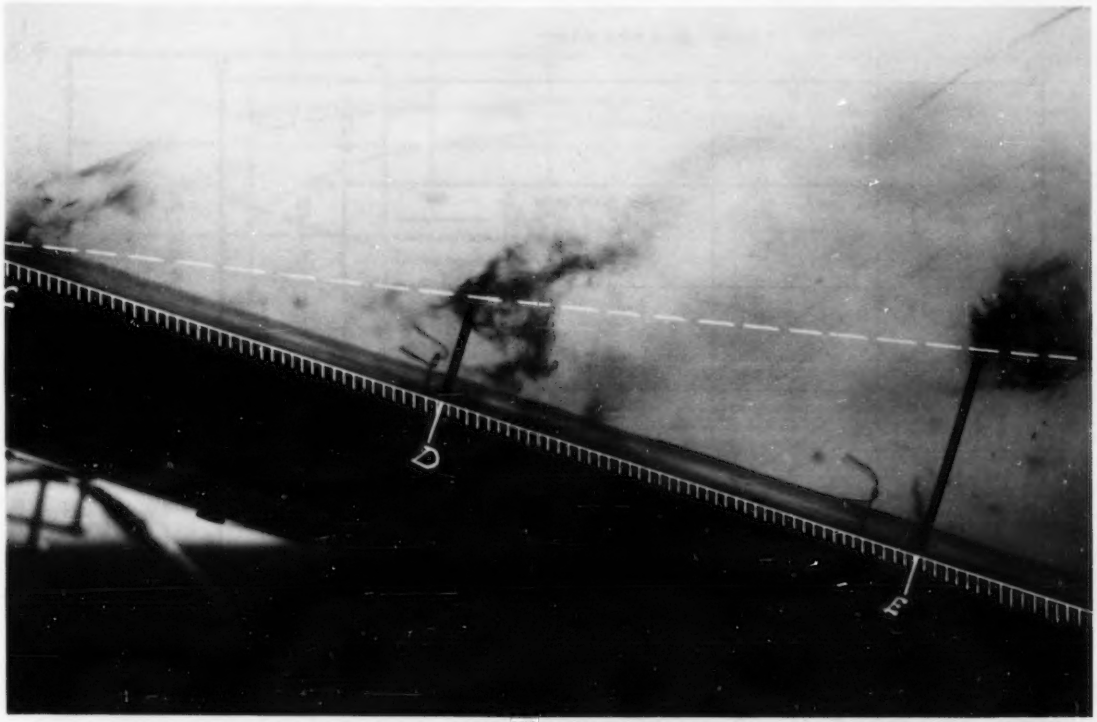

Fig. 10. Separation Boundary at Divergence $\alpha = 18^{o}$ ($R = 1 \times 10^{5}$).

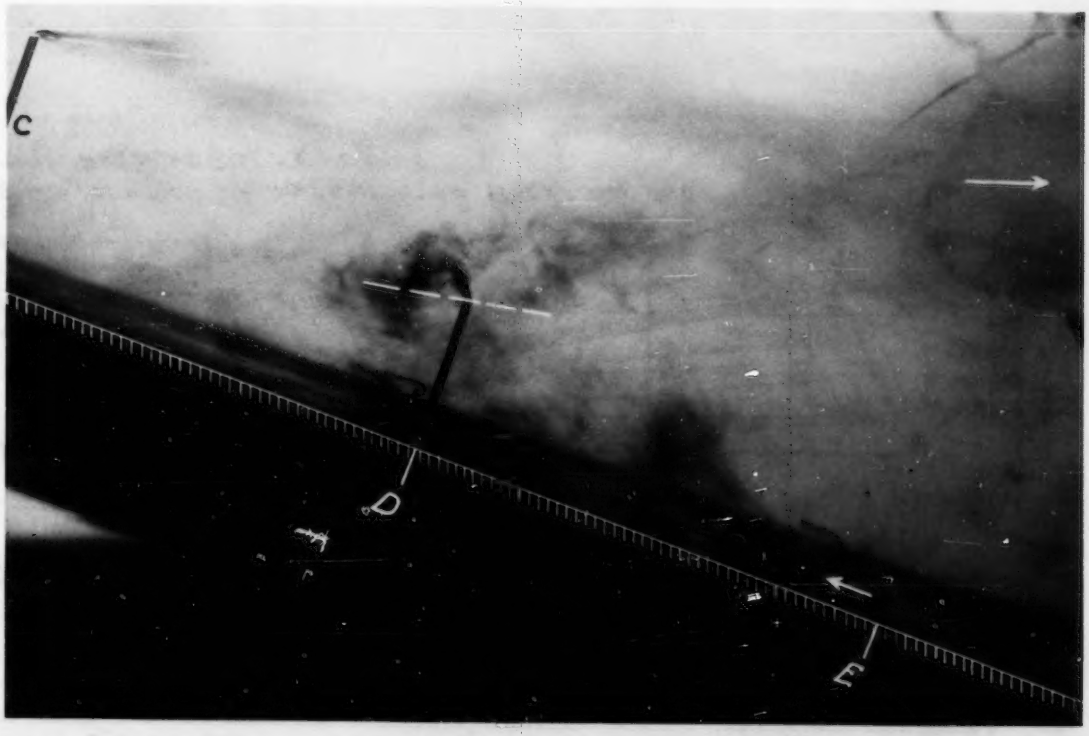

Fig. 11. Separation Phases ($\alpha = 20^{o}$, $R = 1 \times 10^{5}$):
at C - Instant-Stop Boundary
at D - Separation Boundary
at E - Uninterrupted Back-Flow.

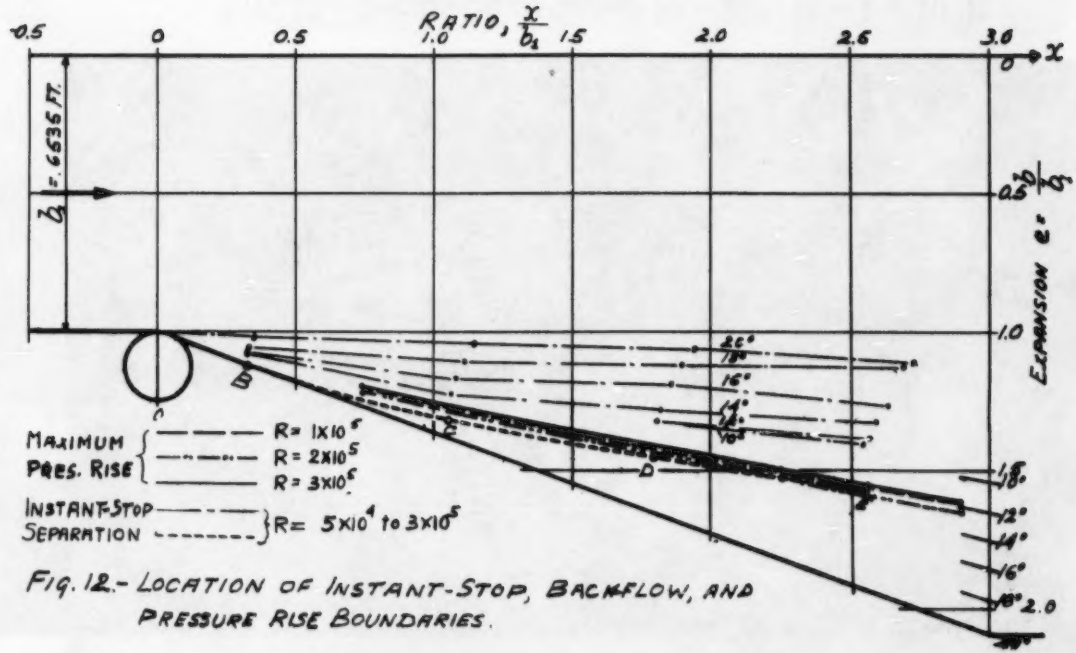

FIG. 12.- LOCATION OF INSTANT-STOP, BACKFLOW, AND PRESSURE RISE BOUNDARIES.

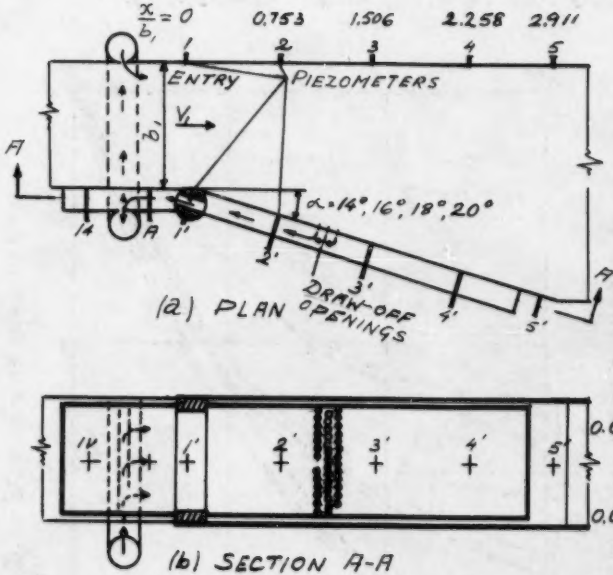

FIG. 13.- SETUP FOR IMPROVEMENT OF PRESSURE RECOVERY

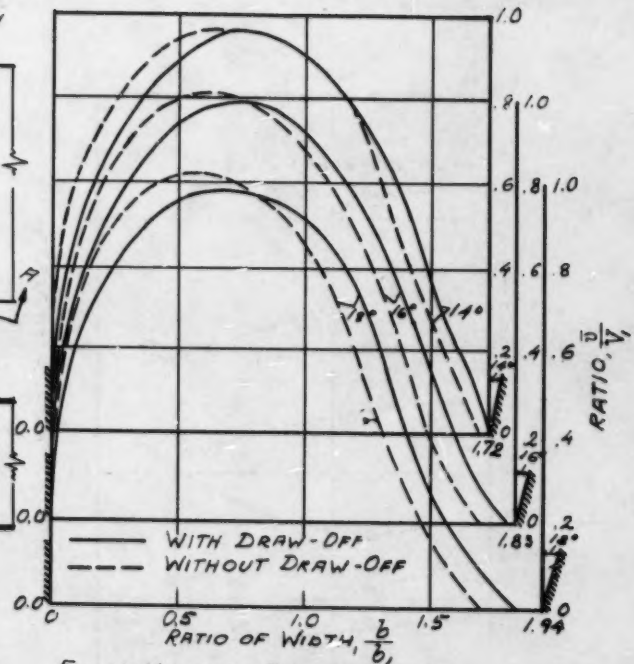

FIG. 14.- VELOCITY DISPLACEMENT

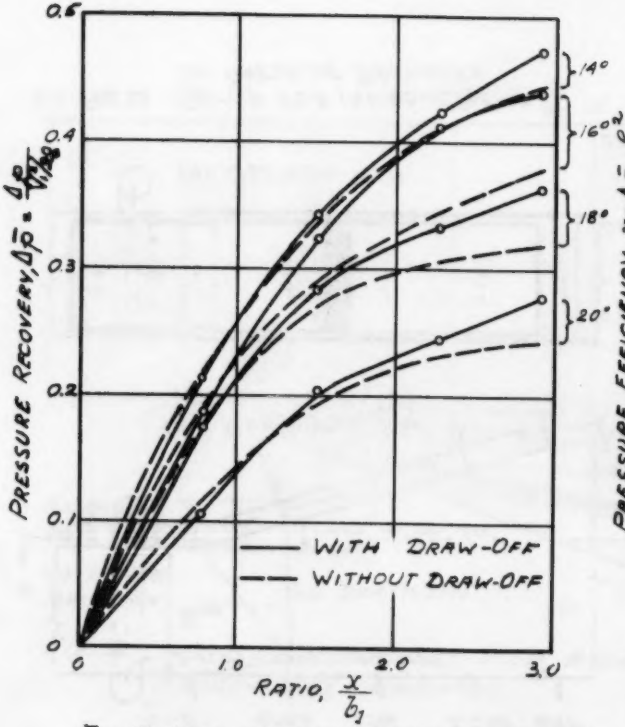

FIG. 15.-IMPROVEMENT OF PRESSURE RECOVERY

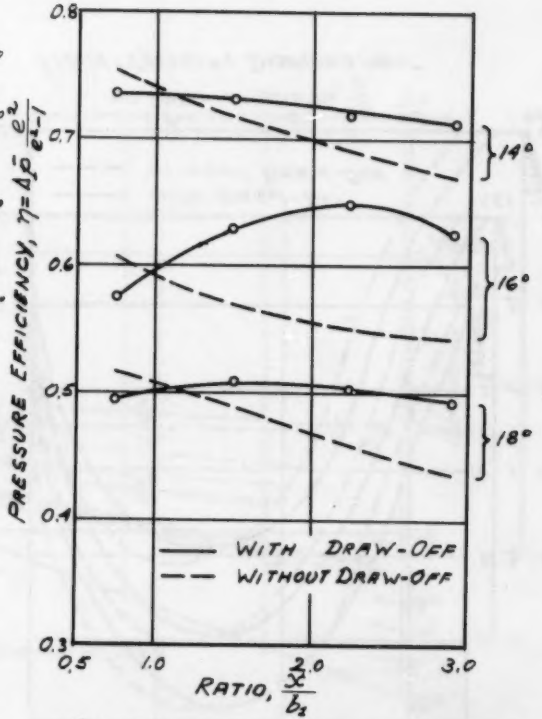

FIG. 16.-IMPROVEMENT OF PRESSURE EFFICIENCY